On the Distribution of the Sum of Double-Nakagami-m Random Vectors and Application in Randomly Reconfigurable Surfaces

Sotiris A. Tegos, *Student Member, IEEE*, Dimitrios Tyrovolas, *Student Member, IEEE*, Panagiotis D. Diamantoulakis, *Senior Member, IEEE*, Christos K. Liaskos, *Member, IEEE*, and George K. Karagiannidis, *Fellow, IEEE*

***Abstract*—Meta-surfaces intend to improve the performance of future wireless networks significantly by controlling the wireless propagation and shaping the radio waves according to the generalized Snell's law. A recent application of meta-surfaces are reconfigurable intelligent surfaces that are mainly proposed for the reflection and steering of the impinging signal. In this article, we introduce randomly reconfigurable surfaces (RRSs) aiming to diffuse the incoming wave and characterize the performance of an RRS-assisted communication network. To facilitate the performance analysis of an RRS-assisted network, first, we present novel closed-form expressions for the probability density function, the cumulative distribution function, the moments, and the characteristic function of the amplitude of the distribution of the sum of double-Nakagami-m random vectors, whose amplitudes follow the double-Nakagami-m distribution, and phases following the circular uniform distribution. We also consider a special case of this distribution, namely the distribution of the sum of Rayleigh-Nakagami-m random vectors. Then, we exploit the obtained expressions to investigate the RRS-assisted composite channel, assuming that the two links undergo Nakagami-m fading. Specifically, closed-form expressions for the outage probability, the average received signal-to-noise ratio, the ergodic capacity, the bit error probability, the amount of fading, and the channel quality estimation index are provided to evaluate the performance of the considered system. Finally, these metrics are also derived for the practical special case where one of the two links undergoes Rayleigh fading, implying that this link is non-line-of-sight.**

***Index Terms*—Diffusion, double-Nakagami-m fading, reconfigurable intelligent surfaces, randomly reconfigurable surfaces.**

Manuscript received October 27, 2021; revised January 30, 2022 and March 15, 2022; accepted March 18, 2022. Date of publication April 5, 2022; date of current version July 18, 2022. The work of Sotiris A. Tegos and George K. Karagiannidis was supported by European Regional Development Fund by European Union and Greek National Funds through Operational Program Competitiveness, Entrepreneurship and Innovation, under the call: Special Actions: Aquaculture - Industrial Materials - Open Innovation in Culture under Project T6YBP-00134. The work of Dimitrios Tyrovolas and Panagiotis D. Diamantoulakis was supported by European Union's Horizon 2020 Research and Innovation Programme under Grant Agreement 957406. The work of Christos K. Liaskos was supported by H2020 Project C4IIoT, under Grant EU833828. The review of this article was coordinated by Dr. Jung-Chieh Chen. *(Corresponding author: Sotiris A. Tegos.)*

Sotiris A. Tegos, Dimitrios Tyrovolas, Panagiotis D. Diamantoulakis, and George K. Karagiannidis are with the Department of Wireless Communications and Information Processing (WCIP) Group, Electrical and Computer Engineering, Aristotle University of Thessaloniki, 54 124 Thessaloniki, Greece (e-mail: tegosoti@auth.gr; tyrovolas@auth.gr; padiaman@auth.gr; geokarag@auth.gr).

Christos K. Liaskos is with the Department of Computer Science Engineering, University of Ioannina, 45110 Ioannina, Greece (e-mail: cliaskos@cse.uoi.gr).

Digital Object Identifier 10.1109/TVT.2022.3164846

I. Introduction

NOWADAYS, the need for higher data rate grows exponentially as the number of smart devices demanding ultra-reliable connection to mobile networks keeps increasing following Edholm's law [1]. The upcoming advent of the sixth generation (6 G) wireless networks requires low latency, coverage extension, improved throughput and security leading to communications on higher frequency bands like millimeter wave (mmWave) and wireless optical communications [2], [3]. The main obstacles of communications in these bands are the sensitivity to blockage due to higher atmospheric attenuation, i.e., severe path loss, leading to limited coverage. One solution for the aforementioned problem is the denser deployment of base stations (BSs) which can fill coverage holes, reduce the path loss, and facilitate higher rates, but with a higher cost and power consumption. To this end, the development of a smart radio environment (SRE) [4] is considered as an operational alternative due to its ability to provide large spectrum bandwidth with lower cost compared to the denser deployment of BSs.

A. Motivation

Until recently, the propagation medium in the field of wireless communications has been perceived as a randomly behaving entity between the communicating systems, which negatively affects the quality of the received signal due to the uncontrollable interactions of the transmitted radio waves with the surrounding objects, e.g., reflections, scattering, etc. [5]. However, in the future SREs, the wireless propagation is envisioned to be controllable and the information processed through the transmission. This is facilitated by the ability of SREs to provide future wireless networks with uninterrupted wireless connectivity using meta-surfaces. Specifically, a meta-surface is an artificial structure with engineered properties, able to alter any impinging electromagnetic wave according to its frequency in a desired way [6], [7]. Practically, a meta-surface is a surface with small but not negligible depth that consists of a two-dimensional array

of sub-wavelength metallic or dielectric scattering elements, where by changing their impedance, the phase profile of the meta-surface can be altered, leading to the transformation of a random incident wave into a specified one. However, to fulfill the vision of the SREs, the properties of a meta-surface should be adjustable in order to provide to the users the required quality of service (QoS).

Reconfigurable intelligent surfaces (RISs) have been introduced as meta-surfaces connected with a controller whose properties can be real-time altered according to the controller's signals and, thus, adjust to the network demands. Each RIS incorporates a lightweight gateway, which enables it to receive commands, and in collaboration with existing beamforming and localization mechanisms, its properties can be appropriately adjusted. In more detail, by altering the RIS properties, it can implement a plethora of electromagnetic functions such as reflection, steering, diffusion, absorption, etc. [7].

RISs have been studied extensively over the last years and have been proven to be able to improve the network's QoS through the steering function if the channel state information (CSI) and user's position are acquired which might not always be the case [8]–[10]. In [11], closed-form expressions for the outage probability and the ergodic capacity for different fading environments were derived assuming RIS-assisted communications with perfect phase estimation. Moreover, [12]–[15] investigated the performance of an RIS-assisted network with phase errors due to imperfect CSI, quantized reflection phases, or both of them. Specifically, in [12] the composite channel of an RIS-assisted system with imperfect phase shifting was proved to be equivalent to a point-to-point Nakagami-m fading channel by invoking the central limit theorem (CLT). However, the CLT does not provide accurate results for an RIS with small number of elements. Furthermore, the authors of [13] derived the probability density function (PDF) of the channel fading coefficients between a BS, an RIS, and a single-antenna user, where the channel amplitude is assumed to follow a double-Nakagami-m distribution, and the phase estimation errors follow the von Mises distribution. However, a closed-form expression for the PDF was not provided. Finally, in [14], the bit error probability of an RIS-assisted system with phase errors was calculated by leveraging the characteristic function estimated through the Gauss-Chebyshev quadrature approximation, while in [15], the error probability and the secrecy outage probability were derived by using the von Mises distribution for the phase errors and the moment-matching technique. Moreover, in [16], an RIS-assisted network is investigated and two phase configuration designs are considered, a random one and one based on coherent phase shifting. However, to describe the performance of the considered network, integral expressions are provided for small number of reflecting elements and CLT approximation is used for large number of reflecting elements. Regarding the fading model, Rayleigh fading is frequently considered for both communication links [5], [17], [18] which is not a legit choice for a practical RIS-assisted communication scenario since RISs are carefully deployed to leverage line-of-sight (LoS) links between the terminals.

Concluding the state-of-the-art, programmable meta-surfaces have various capabilities to perform various electromagnetic functions such as:

- *Steering:* The meta-surface is configured to reflect an impinging wave towards a specific direction.
- *Absorption:* The meta-surface is programmed to fully absorb an impinging wave of given polarization and direction of incidence.
- *Polarization:* The meta-surface modifies the polarization of the impinging wave to either a mix of transverse electric (TE) and transverse magnetic (TM) polarization or one of them.
- *Beamsplitting:* The meta-surface splits the reflected wave in a number of beams at distinct directions, different from the specular reflection direction.
- *Diffusion:* The meta-surface is programmed to diffuse isotropically the impinging radiation.

However, most works propose programmable meta-surfaces only as passive beamformers utilizing the steering function and do not take into consideration their other capabilities and functionalities. In fact, if the user's location is not acquired, it is not optimal to steer the incoming wave to a random point. A possible strategy for such scenarios is to diffuse the incoming electromagnetic waves in the half-space in front of the programmable meta-surface which can be achieved by changing its radiation pattern randomly in every coherence time interval. It should be highlighted that this system does not require the user's location or CSI at the BS. Besides, this electromagnetic function can be useful in multi-user systems where the perfect phase adjustment of RISs may be difficult or even impossible, especially for large number of users, like in massive machine-type communication scenarios [19]. To this end, a programmable meta-surface whose phase profile is altered randomly in every coherence time interval should be utilized for the diffusion of the impinging signal. To the best of the authors' knowledge, the performance of a wireless communication network assisted by a diffusing programmable meta-surface, has not yet been investigated in the existing literature.

B. Contribution

In this paper, we investigate a system assisted by a programmable meta-surface which is utilized to diffuse the impinging signal in the space in front of it. To facilitate the performance analysis of this system, first, we investigate the distribution of the sum of double-Nakagami-m random vectors. Specifically, the contributions of this work are listed below:

- We introduce randomly reconfigurable surfaces (RRSs), being defined as programmable meta-surfaces whose elements induce randomly selected time-variant phase shifts on the reflected signal, in order to diffuse the impinging signal. The proposed blind diffusion manipulation of the impinging waves is intended as an additional capability of a software-programmable meta-surface, when the transmitter or receiver positions are unknown, or CSI derivation loops are not possible.

- We investigate the distribution of the sum of double-Nakagami-m random vectors with amplitudes following the double-Nakagami-m distribution, i.e., the distribution of the product of two random variables (RVs) following the Nakagami-m distribution, and phases that are circular uniformly distributed. Specifically, we provide exact closed-form expressions for the statistical properties of the amplitude of this distribution, i.e., the PDF, the cumulative distribution function (CDF), the moments and the characteristic function. The aforementioned statistical properties are also derived for the distribution of the sum of Rayleigh-Nakagami-m random vectors which is a special case of the former distribution, where the amplitudes of the vectors follow the distribution of the product of an RV following the Rayleigh distribution and one following the Nakagami-m distribution.
- We utilize the derived expressions to investigate a practical RRS-assisted system where Nakagami-m fading channel is assumed between the BS and the RRS and between the RRS and the user. We extract useful metrics to investigate the performance of the considered system, such as the outage probability, the average received signal-to-noise ratio (SNR), which is proved to be proportional to the number of elements, the ergodic capacity, the bit error probability (BEP) for both binary and M-ary modulations, the amount of fading (AoF) and the channel quality estimation index (CQEI). Simplified expressions for these metrics are also provided for the practical special case where one of the links, usually the link between the RRS and the user, is a non-LoS link and undergoes Rayleigh fading. Also, it should be highlighted that the RRS-assisted system's performance can be considered a lower bound of the performance of an RIS-assisted system.

C. Structure

The rest of the paper is organized as follows: in Section II, the statistical properties of the distribution of the sum of double-Nakagami-m random vectors and the distribution of the sum of Rayleigh-Nakagami-m random vectors are provided. In Section III, an RRS-assisted system is investigated, useful performance metrics are provided and numerical results are provided to illustrate the performance of the considered system. Finally, closing remarks and discussion are provided in Section IV.

II. The Distribution of the Sum of Double-Nakagami-m Random Vectors

We consider N double-Nakagami-m random vectors, X_k, $k \in \{1, N\}$, with amplitudes h_k and phases θ_k, i.e.,

$$X_k = h_k e^{j\theta_k}. \tag{1}$$

The amplitudes h_k are independent and identically distributed (i.i.d.) RVs, which follow the double-Nakagami-m distribution with parameters m_1, m_2, Ω_1 and Ω_2, i.e., the distribution of the product of two RVs following the Nakagami-m distribution, whose PDF is given by [20]

$$f_{h_k}(z) = \frac{4z^{m_1+m_2-1}}{\Gamma(m_1)\Gamma(m_2)} \left(\frac{m_1 m_2}{\Omega_1\Omega_2}\right)^{\frac{m_1+m_2}{2}} \times K_{m_1-m_2}\left(2z\sqrt{\frac{m_1 m_2}{\Omega_1\Omega_2}}\right), \tag{2}$$

where $\Gamma(\cdot)$ is the Gamma function [21]. Moreover, the phases θ_k are uniformly distributed in $[0, 2\pi]$.

Next, we define the vector H as

$$H = \sum_{k=1}^{N} X_k. \tag{3}$$

Theorem 1: The PDF of $|H|$ can be expressed in closed-form as

$$f_{|H|}(r) = \sum_{k_1=0}^{m_1-1} \cdots \sum_{k_N=0}^{m_1-1} \prod_{i=1}^{N} \frac{(m_2)_{m_1-1-k_i}(1-m_2)_{k_i}}{(m_1-1-k)!k_i!} \times \frac{4\left(\frac{m_1 m_2}{\Omega_1\Omega_2}\right)^{\frac{u+1}{2}}}{(u-1)!} r^u K_{u-1}\left(2\sqrt{\frac{m_1 m_2}{\Omega_1\Omega_2}}r\right), \tag{4}$$

where $u = N(m_1+m_2-1) - \sum_{i=1}^{N} k_i$, $K_v()$ is the v-th order modified Bessel function of the second kind [21], $(n)_k$ is the Pochhammer symbol and $k!$ is the factorial of k.

Proof: The proof is provided in Appendix A.

It should be highlighted that m_1 and m_2 are used interchangeably. In the following proposition, we present the PDF for a special case, where the amplitudes of the vectors follow the distribution of the product of an RV following the Rayleigh distribution and one following the Nakagami-m distribution, i.e., the distribution of the sum of Rayleigh-Nakagami-m random vectors.

Proposition 1: The PDF of $|H|$, when H follows the distribution of the sum of Rayleigh-Nakagami-m random vectors, can be expressed in closed-form as

$$f_{|H|}(r) = \frac{4\left(\frac{m}{\Omega_1\Omega_2}\right)^{\frac{Nm+1}{2}}}{(Nm-1)!} r^{Nm} K_{Nm-1}\left(2\sqrt{\frac{m}{\Omega_1\Omega_2}}r\right). \tag{5}$$

Proof: Without loss of generality, since in (4) m_1 and m_2 are used interchangeably, we set $m_1 = 1$ and $m_2 = m$ and (5) is derived.

Remark 1: From (5), it can be observed that the distribution of the amplitude of the sum of Rayleigh-Nakagami-m random vectors is a double-Nakagami-m distribution with PDF given by (2) where $m_1 = 1$, $m_2 = Nm$, and replacing Ω_2 with $N\Omega_2$.

In the following theorem, the CDF of the amplitude of the sum of double-Nakagami-m random vectors is derived in closed-form.

Theorem 2: The CDF of $|H|$ can be expressed as

$$F_{|H|}(r) = \sum_{k_1=0}^{m_1-1} \cdots \sum_{k_N=0}^{m_1-1} \prod_{i=1}^{N} \frac{(m_2)_{m_1-1-k_i}(1-m_2)_{k_i}}{(m_1-1-k)!k_i!} \times \left(1 - \frac{2}{(u-1)!}\left(\sqrt{\frac{m_1 m_2}{\Omega_1\Omega_2}}r\right)^u K_u\left(2\sqrt{\frac{m_1 m_2}{\Omega_1\Omega_2}}r\right)\right). \tag{6}$$

Proof: The CDF of $|H|$ is defined as

$$F_{|H|}(r) = \int_0^r f_{|H|}(x)dx. \tag{7}$$

Also, from [22, 03.04.21.0010.01], it stands that

$$\int x^u K_{u-1}(x)dx = -x^u K_u(x). \tag{8}$$

Since $x^u K_u(x)$ is not defined in 0, we utilize the following limit, which we prove in Appendix B,

$$\lim_{x\to 0} x^v K_v(x) = 2^{v-1}(v-1)!, \quad v \in \mathbb{Z}, v > 0 \tag{9}$$

and after some algebraic manipulations, (6) is derived. ■

Next, we provide the CDF of $|H|$ for the considered special case.

Proposition 2: The CDF of $|H|$, when H follows the distribution of the sum of Rayleigh-Nakagami-m random vectors, can be expressed in closed-form as

$$F_{|H|}(r) = 1 - \frac{2}{(Nm-1)!}\left(\sqrt{\frac{m}{\Omega_1\Omega_2}}r\right)^{Nm} \times K_{Nm}\left(2\sqrt{\frac{m}{\Omega_1\Omega_2}}r\right). \tag{10}$$

Proof: Setting $m_1 = 1$ and $m_2 = m$ in (6), (10) is derived.

Next, we derive closed-form expression for the moments of the amplitude of the sum of double-Nakagami-m random vectors.

Theorem 3: The n-th moment of $|H|$ can be formulated as

$$\mu^n = \left(\frac{\Omega_1\Omega_2}{m_1 m_2}\right)^{\frac{n}{2}} \sum_{k_1=0}^{m_1-1}\cdots\sum_{k_N=0}^{m_1-1} \prod_{i=1}^{N} \frac{(m_2)_{m_1-1-k_i}(1-m_2)_{k_i}}{(m_1-1-k)!k_i!} \frac{\Gamma\left(\frac{n}{2}+1\right)\Gamma\left(\frac{n}{2}+u\right)}{\Gamma(u)}. \tag{11}$$

Proof: The n-th moment of $|H|$ is defined as

$$\mu^n = \int_0^\infty x^n f_{|H|}(x)dx. \tag{12}$$

Using [21, 6.561/16] and after some algebraic manipulations, (11) is derived.

Considering the even moments, the l-th moment of $|H|$ with $l = 2n$ can be simplified as

$$\mu^l = \left(\frac{\Omega_1\Omega_2}{m_1 m_2}\right)^{l} \sum_{k_1=0}^{m_1-1}\cdots\sum_{k_N=0}^{m_1-1} \prod_{i=1}^{N} \frac{(m_2)_{m_1-1-k_i}(1-m_2)_{k_i}}{(m_1-1-k)!k_i!} l!(u)_l. \tag{13}$$

In the following proposition, the moments of the considered distribution are derived for the special case.

Proposition 3: The n-th moment of $|H|$, when H follows the distribution of the sum of Rayleigh-Nakagami-m random vectors, can be expressed in closed-form as

$$\mu^n = \left(\frac{\Omega_1\Omega_2}{m}\right)^{\frac{n}{2}} \frac{\Gamma\left(\frac{n}{2}+1\right)\Gamma\left(\frac{n}{2}+Nm\right)}{\Gamma(Nm)}. \tag{14}$$

Proof: Setting $m_1 = 1$ and $m_2 = m$ in (11), (14) is derived.

Considering the even moments for the special case, the l-th moment of $|H|$ can be simplified as

$$\mu^l = \left(\frac{\Omega_1\Omega_2}{m}\right)^{l} l!(Nm)_l. \tag{15}$$

In the following theorem, we derive the characteristic function of the amplitude of the sum of double-Nakagami-m random vectors.

Theorem 4: The characteristic function of $|H|$ can be expressed in closed form as

$$\varphi_{|H|}(t) = \sum_{k_1=0}^{m_1-1}\cdots\sum_{k_N=0}^{m_1-1}\prod_{i=1}^{N} \frac{(m_2)_{m_1-1-k_i}(1-m_2)_{k_i}}{(m_1-1-k)!k_i!} \times \left(\frac{m_1 m_2}{\Omega_1\Omega_2}\right)^{u} \left(\frac{2\sqrt{m_1 m_2}}{\sqrt{\Omega_1\Omega_2}} - jt\right)^{-2u} \frac{2^{4u}}{1+2u} \times {}_2F_1\left(2u, u-\frac{1}{2}, u+\frac{3}{2}, \frac{jt\sqrt{\Omega_1\Omega_2}+2\sqrt{m_1 m_2}}{jt\sqrt{\Omega_1\Omega_2}-2\sqrt{m_1 m_2}}\right), \tag{16}$$

where $t \in \mathbb{R}$ and $j^2 = -1$.

Proof: The characteristic function of $|H|$ is defined as

$$\varphi_{|H|}(t) = \int_0^\infty e^{jtx} f_{|H|}(x)dx. \tag{17}$$

Using [21, 6.621/3] and after some algebraic manipulations, (16) is derived.

In the following proposition, the characteristic function is derived for the considered special case.

Proposition 4: The characteristic function of $|H|$, when H follows the distribution of the sum of Rayleigh-Nakagami-m random vectors, can be expressed in closed-form as

$$\varphi_{|H|}(t) = \left(\frac{m_1 m_2}{\Omega_1\Omega_2}\right)^{Nm} \left(\frac{2\sqrt{m_1 m_2}}{\sqrt{\Omega_1\Omega_2}} - jt\right)^{-2Nm} \frac{2^{4Nm}}{1+2Nm} \times {}_2F_1\left(2Nm, Nm-\frac{1}{2}, Nm+\frac{3}{2}, \frac{jt\sqrt{\Omega_1\Omega_2}+2\sqrt{m_1 m_2}}{jt\sqrt{\Omega_1\Omega_2}-2\sqrt{m_1 m_2}}\right). \tag{18}$$

Proof: Setting $m_1 = 1$ and $m_2 = m$ in (16), (18) is derived. ■

III. Application in Programmable Meta-Surfaces

In this section, we introduce RRSs which induce randomly selected time-variant phase shifts on the reflected signal in order to diffuse the incoming wave, investigate a practical RRS-assisted system and provide useful metrics to evaluate its performance.

A. System Model

We consider a single-input-single-output (SISO) communication system consisting of a BS with a single isotropic antenna,

an RRS and a single user with a single isotropic antenna. The transmitted signal by the BS is reflected randomly from the RRS, consisting of N reflecting elements, and then is received by the user. It is assumed that obstacles, such as buildings, block the direct link from the BS to the user [11], which is a realistic assumption, especially when high-frequency bands are used.The received signal, Y, in the user can be expressed as

$$Y = \sqrt{lpG}\sum_{k=1}^{N} e^{j\phi_k} H_{1k} H_{2k} X + W, \tag{19}$$

where X and W denote the transmitted signal and the additive white Gaussian noise, respectively, and e is the basis of the natural logarithm. The complex channel coefficients between the BS and the RRS and between the RRS and the user are denoted by H_{1k} and H_{2k}, respectively. Moreover, l, p, G and ϕ_k denote the equivalent path loss, the transmitted power, the product of the BS and the user antenna gains G_t and G_r, and the phase adjustment performed by the RRS, respectively. Furthermore, it is assumed that $|H_{1k}|$ and $|H_{2k}|$ are RVs following the Nakagami-m distribution with shape parameters m_1 and m_2, respectively, and spread parameters Ω_1 and Ω_2, respectively, which are the same for all N elements [13]. The PDFs of the envelope and the phase of H_{ik} with $i \in \{1, 2\}$ are given, respectively, by [23]

$$f_{|H_{ik}|}(r) = \frac{2m_i^{m_i} r^{2m_i - 1}}{\Omega_i^{m_i}\Gamma(m_i)} e^{-\frac{m_i r^2}{\Omega_i}} \tag{20}$$

and

$$f_{\arg(H_{ik})}(\tau) = \frac{\Gamma(m_i)|\sin(2\tau)|^{m_i - 1}}{2^{m_i}\Gamma^2(\frac{m_i}{2})}, \tag{21}$$

where $\arg(\cdot)$ denotes the argument of a complex number. It should be highlighted that, in Nakagami fading, the phase of H_{ik} is not uniform, in contrast with Rayleigh fading where the phase follows the uniform distribution.

The k-th element of the RRS induces a phase shift ϕ_k which is uniformly distributed in $[0, 2\pi]$ and is reconfigured per period equal to the coherence time, aiming to diffuse the impinging wave. Considering that the sum of a circular uniform RV with an RV which follows an arbitrary circular distribution results in a circular uniform RV [24], $\theta_k = \phi_k + \arg(H_{1k}) + \arg(H_{2k})$ is uniformly distributed in $[0, 2\pi]$, although $\arg(H_{1k})$ and $\arg(H_{2k})$ are not uniformly distributed. It is obvious that the distribution of θ_k does not depend on the distribution of $\arg(H_{1k})$ and $\arg(H_{2k})$, thus RRSs diffuse the impinging wave regardless of the distribution of the fading. In this case, CSI is not necessary at the BS in an RRS-assisted network which highlights the fact that the considered system is less complex than an RIS-assisted network.

It should also be highlighted that the effective utilization of multiple antennas is based on the perfect knowledge of CSI in order to form the optimal beamforming vector, which determines how the available power is split among the antennas of the BS. When no CSI is available at the BS, which is the case in the proposed RRS-assisted network, the only reasonable transmit strategy is to spread the power omnidirectionally among the antennas [25]. Therefore, using multiple antennas will not result in major improvement in the considered system, since the main advantage of multiple antennas, i.e., the beamforming gain, is not utilized.

Furthermore, in RIS-assisted systems, the RIS attempts to cancel the phase introduced by the product of the two complex channel coefficients with the use of the phase shift ϕ_k. Practically, the phase correction is not perfect resulting in a phase error θ_k which is frequently modeled as an RV following the von Mises distribution with concentration parameter κ [12]. If $\kappa = 0$, the distribution of the phase error θ_k is uniform and for small values of κ the distribution is close to uniform. When $\kappa = 0$, the phase errors are equally probable, thus the performance achieved in the RRS-assisted system can be considered as a lower bound of the performance of an RIS-assisted system.

Therefore, the received signal in (19) can be expressed as

$$Y = \sqrt{lp}\sum_{k=1}^{N} e^{j\theta_k}|H_{1k}||H_{2k}|X + W. \tag{22}$$

We define the composite channel coefficient H as

$$H = \sum_{k=1}^{N} e^{j\theta_k}|H_{1k}||H_{2k}|. \tag{23}$$

Therefore, the PDF of the composite channel coefficient $|H|$ is given by (4), since H follows the distribution of the sum of i.i.d. double-Nakagami-m random vectors [11], [13]. Also, it should be highlighted that if one of the two links, usually the link between the RRS and the user, is a non-LoS link, Rayleigh fading can be used to describe the channel conditions of this link, thus the PDF of the composite channel coefficient $|H|$ is given by (5), since H follows the distribution of the sum of i.i.d. Rayleigh-Nakagami-m random vectors.

B. Performance Evaluation

In this subsection, the performance of the considered system is evaluated in terms of the outage probability, the average received SNR, the ergodic capacity, the BEP, the AoF and the CQEI.

Corollary 1: The outage probability can be obtained through (6) as

$$P_o = F_{|H|}\left(\sqrt{\frac{\gamma_{\text{thr}}}{l\gamma_t}}\right), \tag{24}$$

where γ_t denotes the transmitted SNR and γ_{thr} denotes the threshold which defines the outage.

If we consider the special case where one link follows the Nakagami-m distribution and the other link follows the Rayleigh distribution, the outage probability can be expressed using (10).

In the following proposition, the average received SNR is provided and is proved to be independent of m_1 and m_2, thus it can be utilized for both considered cases.

Proposition 5: The average received SNR is given by

$$\mathbb{E}[\gamma_r] = lN\Omega_1\Omega_2\gamma_t. \tag{25}$$

Proof: The average received SNR can be obtained as

$$\mathbb{E}[\gamma_r] = l\mathbb{E}\left[|H|^2\right]\gamma_t, \tag{26}$$

where $\mathbb{E}[|H|^2]$ is the expected value of the channel gain which can be derived as the second moment in (11), i.e.,

$$\mathbb{E}\left[|H|^2\right] = \frac{\Omega_1\Omega_2}{m_1 m_2}\sum_{k_1=0}^{m_1-1}\cdots\sum_{k_N=0}^{m_1-1}\prod_{i=1}^{N}\frac{(m_2)_{m_1-1-k_i}(1-m_2)_{k_i}}{(m_1-1-k)!k_i!}u. \quad (27)$$

Using [22, 06.10.16.0005.01] and the fact that $(1)_n = n!$, $n \in \mathbb{Z}, n > 0$, it is proven that

$$\sum_{k_i=0}^{m_1-1}\frac{(m_2)_{m_1-1-k_i}(1-m_2)_{k_i}}{(m_1-1-k)!k_i!} = 1. \quad (28)$$

Moreover, using [22, 06.10.17.0002.02], it is proven that

$$k_i(1-m_2)_{k_i} = (1-m_2)\left((2-m_2)_{k_i} - (1-m_2)_{k_i}\right). \quad (29)$$

Also, using (28) and (29), it can be proven that

$$\sum_{k_i=0}^{m_1-1}\frac{k_i(m_2)_{m_1-1-k_i}(1-m_2)_{k_i}}{(m_1-1-k)!k_i!} = (1-m_2)(m_1-1). \quad (30)$$

Utilizing (28) and (30) and after some algebraic manipulations, (25) is derived.

Remark 2: As it is can be observed in (25), the average received SNR is proportional to the number of reflecting elements N, since the power impinges upon N reflecting elements and then is diffused.

Next, we provide the ergodic capacity of the considered system.

Proposition 6: The ergodic capacity can be expressed as

$$C = \frac{B}{\ln 2}\sum_{k_1=0}^{m_1-1}\cdots\sum_{k_N=0}^{m_1-1}\prod_{i=1}^{N}\frac{(m_2)_{m_1-1-k_i}(1-m_2)_{k_i}}{(m_1-1-k)!k_i!} \times \frac{1}{(u-1)!}G_{3,1}^{1,3}\left(\frac{l\gamma_t\Omega_1\Omega_2}{m_1 m_2}\middle|\begin{matrix}1,1,1-u\\1\end{matrix}\right), \quad (31)$$

where B denotes the bandwidth of the fading channel.

Proof: The ergodic capacity is calculated as the average capacity and is given by

$$C = B\int_0^\infty \log_2\left(1+l\gamma_t r^2\right) f_{|H|}(r)dr. \quad (32)$$

Transforming $\ln(1+x)$ into Meijer's G-function [22, 01.04.26.0002.01] and using [22, 03.04.26.0037.01] and [26], the ergodic capacity can be evaluated as

$$C = \frac{B}{\ln 2}\sum_{k_1=0}^{m_1-1}\cdots\sum_{k_N=0}^{m_1-1}\prod_{i=1}^{N}\frac{(m_2)_{m_1-1-k_i}(1-m_2)_{k_i}}{(m_1-1-k)!k_i!} \times \frac{1}{(u-1)!}G_{4,2}^{1,4}\left(\frac{l\gamma_t\Omega_1\Omega_2}{m_1 m_2}\middle|\begin{matrix}1,1,1-u,0\\1,0\end{matrix}\right). \quad (33)$$

Using [22, 07.34.04.0002.01] and [22, 07.34.03.0001.01], the Meijer's G-function can be simplified and (31) is derived, which completes the proof.

TABLE I
VALUES OF a AND b IN (35) FOR DIFFERENT BINARY MODULATIONS

Modulation	a	b
BPSK	1	$\frac{1}{2}$
DBPSK	1	1
BFSK	$\frac{1}{2}$	$\frac{1}{2}$
NBFSK	$\frac{1}{2}$	1

TABLE II
VALUES OF τ_M, a_M AND b_k IN (38) FOR DIFFERENT MODULATIONS WITH $M \geq 4$

Modulation	τ_M	a_M	b_k
M-QAM	$\frac{\sqrt{M}}{2}$	$\frac{2}{\log_2 M}\left(1-\frac{1}{\sqrt{M}}\right)$	$\frac{3\log_2 M}{2(M-1)}(2k-1)^2$
M-PSK	$\max\left(\frac{M}{4},1\right)$	$\frac{1}{\max(\log_2 M,2)}$	$\log_2 M\sin^2\left(\frac{2k-1}{M}\pi\right)$

For the considered special case, the ergodic capacity can be expressed as

$$C = \frac{B}{\ln 2(Nm-1)!}G_{3,1}^{1,3}\left(\frac{l\gamma_t\Omega_1\Omega_2}{m}\middle|\begin{matrix}1,1,1-Nm\\1\end{matrix}\right). \quad (34)$$

Next, we provide the BEP of the RRS-assisted system for binary modulations, i.e., binary phase-shift keying (BPSK), differential binary phase-shift keying (DBPSK), binary frequency-shift keying (BFSK) and noncoherent binary frequency-shift keying (NBFSK). In this case, the BEP is given by [27]

$$P_e^b(H) = \frac{1}{2\Gamma(b)}\Gamma\left(b, al|H|^2\gamma_t\right), \quad (35)$$

where a and b are modulation-dependent parameters which are presented in Table I and $\Gamma(\cdot,\cdot)$ is the upper incomplete Gamma function [21].

Proposition 7: The BEP for binary modulations is given by

$$P_e^b = \frac{1}{2\Gamma(b)}\sum_{k_1=0}^{m_1-1}\cdots\sum_{k_N=0}^{m_1-1}\prod_{i=1}^{N}\frac{(m_2)_{m_1-1-k_i}(1-m_2)_{k_i}}{(m_1-1-k)!k_i!} \times \frac{1}{(u-1)!}G_{3,2}^{2,2}\left(\frac{al\gamma_t\Omega_1\Omega_2}{m_1 m_2}\middle|\begin{matrix}1-u,0,1\\0,b\end{matrix}\right). \quad (36)$$

Proof: Transforming $\Gamma(b,x)$ into Meijer's G-function [22, 06.06.26.0005.01] and using [22, 03.04.26.0037.01] and [26], (36) is derived, which completes the proof.

For the considered special case, the BEP for binary modulations can be obtained as

$$P_e^b = \frac{1}{2\Gamma(b)(Nm-1)!}G_{3,2}^{2,2}\left(\frac{al\gamma_t\Omega_1\Omega_2}{m}\middle|\begin{matrix}1-Nm,0,1\\0,b\end{matrix}\right). \quad (37)$$

Next, we provide the BEP of the RRS-assisted system considering M-ary modulations with $M \geq 4$, i.e., quadrature amplitude modulation (QAM) and PSK. In this case, considering that Gray mapping is used, the BEP is given by [28]

$$P_e(H) = a_M\sum_{k=1}^{\tau_M}\text{erfc}\left(\sqrt{b_k l\gamma_t}|H|\right), \quad (38)$$

where a_M, τ_M and b_k are modulation-dependent parameters which are presented in Table II.

Proposition 8: The BEP for M-ary modulations can be expressed as

$$P_e = \frac{1}{\sqrt{\pi}} \sum_{k=1}^{\tau_M} \sum_{k_1=0}^{m_1-1} \cdots \sum_{k_N=0}^{m_1-1} \prod_{i=1}^{N} \frac{(m_2)_{m_1-1-k_i}(1-m_2)_{k_i}}{(m_1-1-k)!k_i!} \times \frac{1}{(u-1)!} G_{3,2}^{2,2}\left(\frac{b_k l \gamma_t \Omega_1 \Omega_2}{m_1 m_2} \Big| \begin{matrix} 1-u, 0, 1 \\ 0, \frac{1}{2} \end{matrix} \right). \quad (39)$$

Proof: Transforming $\mathrm{erfc}(x)$ into Meijer's G-function [22, 06.27.26.0006.01] and using [22, 03.04.26.0037.01] and [26], (39) is derived, which completes the proof. ■

For the considered special case, the BEP for M-ary modulations can be obtained as

$$P_e = \frac{1}{\sqrt{\pi}(Nm-1)!} \sum_{k=1}^{\tau_M} G_{3,2}^{2,2}\left(\frac{b_k l \gamma_t \Omega_1 \Omega_2}{m} \Big| \begin{matrix} 1-Nm, 0, 1 \\ 0, \frac{1}{2} \end{matrix} \right). \quad (40)$$

Next, we present the AoF, a useful performance metric for the analysis of wireless communication systems which is used to quantify the severity of fading and is defined as the ratio of the variance to the square average of the instantaneous received SNR, i.e., [29], [30]

$$\mathrm{AoF} = \frac{\mathbb{E}\left[\gamma_r^2\right] - \left(\mathbb{E}\left[\gamma_r\right]\right)^2}{\left(\mathbb{E}\left[\gamma_r\right]\right)^2}. \quad (41)$$

In the considered RRS-assisted system, the AoF is calculated in the following proposition

Proposition 9: The AoF is given by

$$\mathrm{AoF} = 1 + \frac{1 + m_1 + m_2 - m_1 m_2}{N m_1 m_2}. \quad (42)$$

Proof: The proof is provided in Appendix C. ■

For the considered special case, (42) can be further simplified as

$$\mathrm{AoF} = \frac{2 + Nm}{Nm}. \quad (43)$$

Remark 3: It should be highlighted that for both considered cases, as $N \to \infty$, the AoF tends to 1, which is the value of the AoF for a single Rayleigh channel.

Next, we provide another useful performance metric, the CQEI, which is an improved long-term performance criterion for wireless systems operating over fading channels, assesses the error performance of a communication system efficiently considering the average received SNR and is defined as the ratio of the variance to the cubed mean of the instantaneous received SNR, i.e., [31]

$$\mathrm{CQEI} = \frac{\mathbb{E}\left[\gamma_r^2\right] - \left(\mathbb{E}\left[\gamma_r\right]\right)^2}{\left(\mathbb{E}\left[\gamma_r\right]\right)^3}. \quad (44)$$

In the following proposition, the CQEI is extracted.

Proposition 10: The CQEI can be expressed as

$$\mathrm{CQEI} = \frac{1 + m_1 + m_2 + m_1 m_2 (N-1)}{N^2 m_1 m_2 \Omega_1 \Omega_2 \, l \gamma_t}. \quad (45)$$

Proof: Considering that (44) can be written as

$$\mathrm{CQEI} = \frac{\mathrm{AoF}}{\mathbb{E}\left[\gamma_r\right]}, \quad (46)$$

CQEI can be directly derived from (25) and (42). ■

For the considered special case, (45) can be further simplified as

$$\mathrm{CQEI} = \frac{2 + Nm}{N^2 \, m \Omega_1 \Omega_2 \, l \gamma_t}. \quad (47)$$

C. Numerical Results and Discussion

In this subsection, we illustrate the performance of the considered system. Assuming that both the BS and the user are located at the far field region of the RRS, the equivalent path loss l is given by $l = l_1 l_2$, where l_1 and l_2 denote the path loss of the link between the BS and the RRS and the link between the RRS and the user, respectively. The path loss of each link is modeled as [32]

$$l_i = C_0 \left(\frac{d_i}{d_0} \right)^{-\alpha_i}, \quad (48)$$

where C_0 denotes the reference path loss at the reference distance d_0, d_i, $i \in \{1, 2\}$ denotes the distance of the i-th link and α_i denotes the path loss exponent of the i-th link. We set $m_1 = 3$, $m_2 = 1$, $\Omega_1 = 1$ and $\Omega_2 = 1$, which corresponds to a scenario where there is a LoS link between the BS and the RRS and a non-LoS link between the RRS and the user. This scenario is motivated by the mobility of the user and, thus, the difficulty of establishing a LoS link [18]. Moreover, we also examine the setup where $m_1 = 1$ and $m_2 = 1$ to illustrate a performance lower bound representing a scenario where the RRS is randomly deployed since there is no LoS link. For both path loss links, we set $C_0 = -30$ dB, $d_0 = 1$m, and the path loss exponent for the link between the BS and the RRS and the link between the RRS and the user is set as $\alpha_1 = 2.8$ and $\alpha_2 = 2.2$, respectively [32]. Furthermore, unless stated otherwise, the transmitted SNR is 110 dB, and it is assumed that the sum of the two distances is constant, i.e., $d_1 + d_2 = d$ with $d = 30$m. It is also assumed that as the number of elements increases, the size of the RRS also increases since the inter-distance between them remains unchanged.

Fig. 1 illustrates the impact of the ratio of the transmitted SNR to the outage threshold in the receiver and the number of elements of the RRS on the outage probability. In this figure, we set the distance between the BS and the RRS as $d_1 = 25$m and the distance between the RRS and the user is set as $d_2 = 5$m. It is observed that as the number of elements increases the outage probability decreases, thus it is clear that the QoS can be improved by increasing the number of elements without increasing the power consumption of the transceiver. Specifically, it can be observed that by doubling the number of elements, the same outage performance can be achieved with 3 dB smaller transmitted SNR. However, to significantly improve the outage probability, the size of the RRS must be noticeably large, as in this way more electromagnetic power density will impinge upon

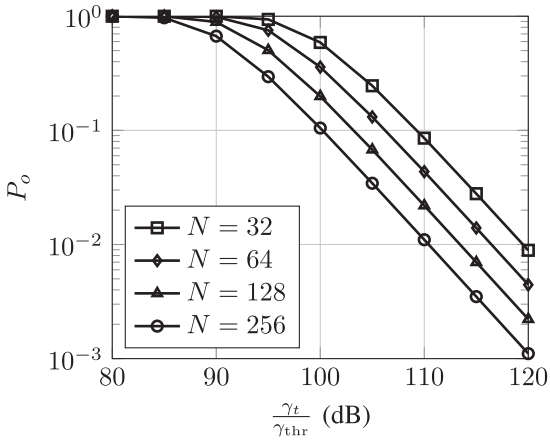

Fig. 1. Outage probability P_o versus $\frac{\gamma_t}{\gamma_{\text{thr}}}$.

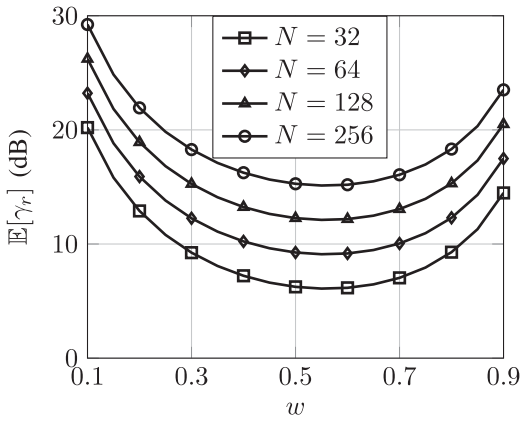

Fig. 2. Average received SNR versus w.

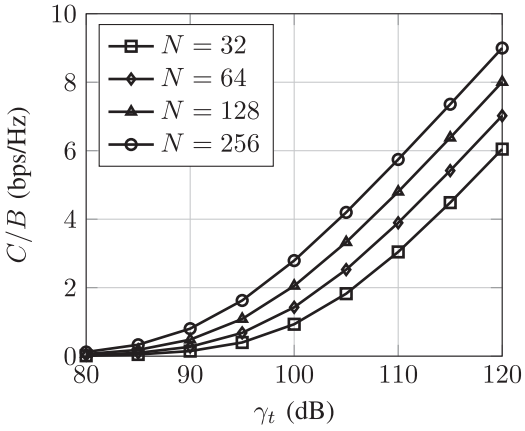

Fig. 3. Normalized ergodic capacity $\frac{C}{B}$ versus γ_t.

the surface and, thus, more energy will be focused on the user leading to an increase of the received SNR.

In Fig. 2 and Fig. 4, we set $d_1 = wd$ and $d_2 = (1-w)d$, where $w \in [0.1, 0.9]$ to ensure that the terminals are located at the far-field region, and the average received SNR and the BEP versus w are illustrated, respectively. For the BEP, the modulation is assumed to be either BPSK or 4-QAM with Gray mapping. It is observed that as the number of elements increases, both the average received SNR and the BEP increases at a certain

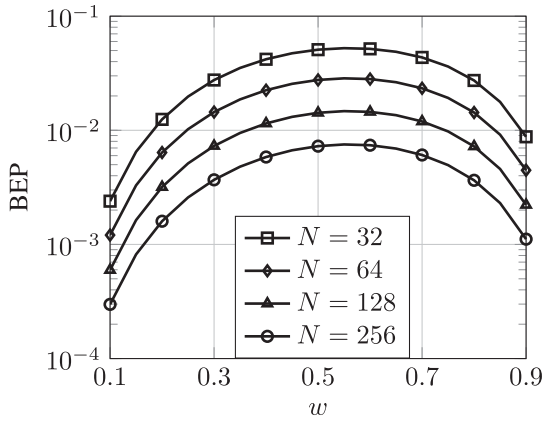

Fig. 4. BEP versus w for BPSK or 4-QAM modulation with Gray mapping.

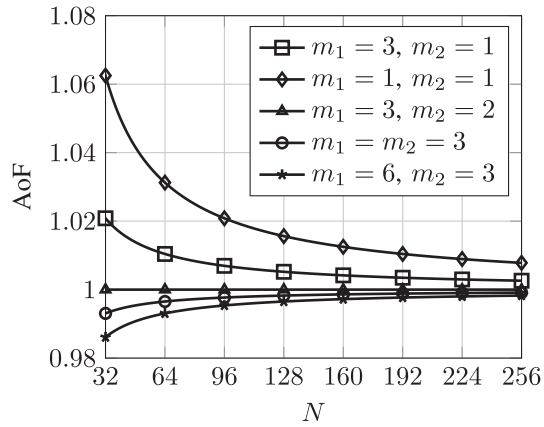

Fig. 5. AoF versus the number of elements N.

distance. Moreover, it should be highlighted that the placement of the RRS plays an important role and it becomes evident that it should be placed either close to the BS or close to the user, since the path losses are maximized when the RRS is placed in an intermediate point between the BS and the user. Also, the fact that the performance is slightly improved when the RRS is placed close to the BS is justified as the exponent a_1 is larger than a_2.

Fig. 3 depicts the impact of the transmitted SNR on the ergodic capacity for different numbers of elements of the RRS. The distances of the two links are set as in Fig. 1. It is observed that high transmitted SNR values are required for successful information transmission. Moreover, increasing the number of elements leads to better ergodic capacity, since the average received SNR is proportional to the number of elements, and the QoS can be improved by the enlargement of the RRS without consuming more power.

Fig. 5 illustrates how the AoF is affected by the number of elements of the RRS. As the number of elements increases, the AoF converges to 1. Especially for the case where $m_1 = 3$ and $m_2 = 2$ the amount of fading equals to 1 regardless of the number of elements. As the number of elements increases, due to the fact that phase shifts are circular uniformly distributed, more non-coherent paths are created. Therefore, when a large RRS with arbitrary phase shift is deployed between two terminals, the AoF tends to 1, which coincides to the value of the AoF

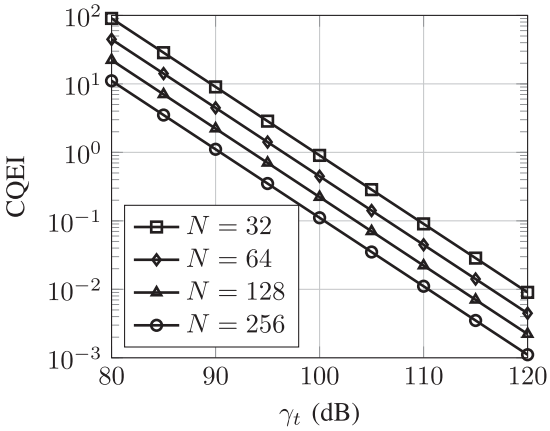

Fig. 6. CQEI versus γ_t.

for a single Rayleigh channel. Moreover, as the AoF is hardly affected by the fading conditions for large number of elements, it follows that the fading conditions have limited impact on the performance of the considered system. It should be highlighted that as m_1 and m_2 are used interchangeably, the AoF is the same for the scenarios where the value of the shape parameters of both links is interchanged, e.g., $\text{AoF}_{3,1} = \text{AoF}_{1,3}$.

Fig. 6 depicts the behavior of the CQEI as the transmitted SNR increases. It should be highlighted that the performance improves as the CQEI decreases. It is clear that as the number of elements increases, the CQEI decreases without requiring larger transmitted SNR and as a consequence the system performance upgrades.

IV. Conclusion

In this work, we have introduced RRSs, being defined as programmable meta-surfaces whose elements induce a randomly selected time-variant phase shift on the reflected signal in order to approximate the diffusion function of a RIS. We have utilized the distribution of the sum of double-Nakagami-m random vectors in an RRS-assisted system where the two links undergo Nakagami-m fading and equivalent phases following the circular uniform distribution are considered. We have derived closed-form expressions of valuable metrics such as the outage probability, the average received SNR, the ergodic capacity, the BEP, the AoF, and the CQEI. It has been proved that the average received SNR is proportional to the number of elements N and it can be observed that a large number of elements is required to improve the system performance. Furthermore, we can enhance the system performance by deploying the RRS in the vicinity of the BS or the user. Finally, it has been illustrated that when a large RRS with arbitrary phase shifts is deployed between two terminals, the AoF tends to 1, which coincides with the value of the AoF for a single Rayleigh channel.

Appendix A
Proof of Theorem 1

The PDF of $|H|$ is given by [33]

$$f_{|H|}(r) = r\int_0^\infty \rho J_0(r\rho)\Lambda(\rho)d\rho, \tag{49}$$

where $J_v()$ is the v-th order Bessel function of the first kind [21] and $\Lambda(\rho)$ can be expressed as

$$\Lambda(\rho) = \mathbb{E}_{h_1\ldots h_N}\left[\prod_{i=1}^{N} J_0(h_i\rho)\right] = \prod_{i=1}^{N}\mathbb{E}_{h_i}\left[J_0(h_i\rho)\right]. \tag{50}$$

The expected value in (50) can be evaluated as

$$\mathbb{E}_{h_i}\left[J_0(h_i\rho)\right] = \int_0^\infty J_0(z\rho)f_{h_i}(z)dz, \tag{51}$$

since $h_1,\ldots,h_N$ are independent. Transforming the Bessel functions into Meijer's G-functions [22, 03.04.26.0037.01], [22, 03.01.26.0056.01] and using [26], (51) can be written as

$$\mathbb{E}_{h_i}\left[J_0(h_i\rho)\right] = \frac{1}{\Gamma(m_1)\Gamma(m_2)} \times G_{2,2}^{1,2}\left(\frac{\Omega_1\Omega_2\rho^2}{4m_1m_2}\middle|\begin{matrix}1-m_1, 1-m_2\\ 0, 0\end{matrix}\right), \tag{52}$$

where $G[\cdot]$ is the Meijer's G-function [21]. Using [22, 07.23.26.0004.01], (52) can be expressed as

$$\mathbb{E}_{h_i}\left[J_0(h_i\rho)\right] = {}_2F_1\left(m_1, m_2; 1; -\frac{\Omega_1\Omega_2\rho^2}{4m_1m_2}\right), \tag{53}$$

where ${}_2F_1(\cdot,\cdot,\cdot,\cdot)$ is the Gauss hypergeometric function [21]. Using [22, 07.23.17.0046.01], the hypergeometric function can be expressed as a finite sum and (53) can be rewritten as

$$\mathbb{E}_{h_i}\left[J_0(h_i\rho)\right] = \frac{(m_1)_{m_2-1}}{(m_2-1)!}\sum_{k=0}^{m_1-1}\frac{(1-m_1)_k(1-m_2)_k}{(2-m_1-m_2)_k k!} \times \left(\frac{4m_1m_2}{4m_1m_1+\Omega_1\Omega_2\rho^2}\right)^{m_1+m_2-k-1}. \tag{54}$$

Considering that all N vectors have the same m_1, m_2, Ω_1 and Ω_2, using (49) and (54) and after some algebraic manipulations similar to [34], the PDF of $|H|$ is given by

$$f_{|H|}(r) = r\left(\frac{(m_1)_{m_2-1}}{(m_2-1)!}\right)^N \sum_{k_1=0}^{m_1-1}\cdots\sum_{k_N=0}^{m_1-1}\left(\frac{4m_1m_2}{\Omega_1\Omega_2}\right)^u \times \int_0^\infty \rho J_0(r\rho)\left(\frac{1}{\frac{4m_1m_2}{\Omega_1\Omega_2}+\rho^2}\right)^u d\rho. \tag{55}$$

It should be highlighted that $u\in\mathbb{Z}, u>0$, since $m_1, m_2\in\mathbb{Z}$. Utilizing [21, 6.565/4] in (55) and after some algebraic manipulations, (4) is derived and the proof is completed.

Appendix B
Proof of (9)

Using L'Hospital's rule and [22, 03.04.20.0005.01], it stands that

$$\lim_{x\to 0}\frac{K_v(x)}{x^{-v}} = -\lim_{x\to 0}\frac{K_v(x)}{x^{-v}} + \lim_{x\to 0}\frac{x^{v+1}}{v}K_{v+1}(x). \tag{56}$$

Thus, the following expression stands

$$2v\lim_{x\to 0}x^vK_v(x) = \lim_{x\to 0}x^{v+1}K_{v+1}(x). \tag{57}$$

Using (57) and considering that $v \in \mathbb{Z}, v > 0$, the following expression can be derived

$$\lim_{x\to 0} x^v K_v(x) = 2^{v-1}(v-1)! \lim_{x\to 0} xK_1(x). \tag{58}$$

An approximation of $K_v(x)$ as $x \to 0$, if $\mathrm{Re}\{v\} > 0$, where $\mathrm{Re}\{\cdot\}$ denotes the real part of a complex number, is given by [35]

$$K_v(x) \simeq \frac{1}{2}\Gamma(v)\left(\frac{1}{2}x\right)^{-v}. \tag{59}$$

Hence, the following limit can be derived

$$\lim_{x\to 0} xK_1(x) = 1. \tag{60}$$

Utilizing (58) and (60), the proof is completed.

Appendix C
Proof of Proposition 9

To prove (42), $\mathbb{E}[\gamma_r^2]$ should be calculated, since $\mathbb{E}[\gamma_r]$ can be obtained from (25). The second moment of the received SNR can be obtained as

$$\mathbb{E}[\gamma_r^2] = l^2 \mathbb{E}\left[|H|^4\right] \gamma_t^2, \tag{61}$$

where $\mathbb{E}[|H|^4]$ can be derived as the fourth moment in (11), i.e.,

$$\mathbb{E}\left[|H|^4\right] = 2\left(\frac{\Omega_1\Omega_2}{m_1 m_2}\right)^2 \sum_{k_1=0}^{m_1-1} \cdots \sum_{k_N=0}^{m_1-1} \prod_{i=1}^{N} \frac{(m_2)_{m_1-1-k_i}(1-m_2)_{k_i}}{(m_1-1-k)!k_i!} u(u+1). \tag{62}$$

Utilizing the proof of Proposition 5, (62) can be written as

$$\mathbb{E}\left[|H|^4\right] = 2\left(\frac{\Omega_1\Omega_2}{m_1 m_2}\right)^2 \sum_{k_1=0}^{m_1-1} \cdots \sum_{k_N=0}^{m_1-1} \prod_{i=1}^{N} \frac{(m_2)_{m_1-1-k_i}(1-m_2)_{k_i}}{(m_1-1-k)!k_i!} u^2 - 2N\frac{\Omega_1^2\Omega_2^2}{m_1 m_2}. \tag{63}$$

The first term in (63), termed as T, considering the definition of u can be written as

$$T_1 = 2\sum_{k_1=0}^{m_1-1} \cdots \sum_{k_N=0}^{m_1-1} \prod_{i=1}^{N} \frac{(m_2)_{m_1-1-k_i}(1-m_2)_{k_i}}{(m_1-1-k)!k_i!} \times \left((N(m_1+m_2-1))^2 - 2N(m_1+m_2-1)\sum_{i=1}^{N} k_i + \left(\sum_{i=1}^{N} k_i\right)^2 \right) \left(\frac{\Omega_1\Omega_2}{m_1 m_2}\right)^2. \tag{64}$$

The first and the second term in (64) can be calculated utilizing the proof of Proposition 5. Using [22, 06.10.17.0002.02] and (29), it is proven that

$$k_i^2(1-m_2)_{k_i} = (1-m_2)\left((2-m_2)(3-m_2)_{k_i} - (3-2m_2)(2-m_2)_{k_i} + (1-m_2)_{k_i}\right). \tag{65}$$

Using (28), (30) and (65), it can be proven that

$$\sum_{k_i=0}^{m_1-1} \frac{k_i^2 (m_2)_{m_1-1-k_i}(1-m_2)_{k_i}}{(m_1-1-k)!k_i!} = (1-m_2) \times \left((2-m_2)\frac{m_1(m_1+1)}{2} - (3-2m_2)m_1 + 1 - m_2\right). \tag{66}$$

Utilizing (28), (30) and (66) and after some algebraic manipulations, the third term in (64), termed as T_2, can be calculated as

$$T_2 = 2\left(\frac{\Omega_1\Omega_2}{m_1 m_2}\right)^2 N\left(\frac{(m_1-1)(m_2-1)}{2}(2-2m_2 + m_1(m_2-2)) + (N-1)((1-m_2)(m_1-1))^2\right). \tag{67}$$

Using (67) and after some algebraic manipulations, (42) can be derived which completes the proof.

References

[1] S. Cherry, "Edholm's law of bandwidth," *IEEE Spectr.*, vol. 41, no. 7, pp. 58–60, Jul. 2004.

[2] C. Pan *et al.*, "Reconfigurable intelligent surfaces for 6G and beyond: Principles, applications, and research directions," 2020. [Online]. Available: https://arxiv.org/abs/2011.04300

[3] A. Yadav and O. A. Dobre, "All technologies work together for good: A glance at future mobile networks," *IEEE Wireless Commun.*, vol. 25, no. 4, pp. 10–16, Aug. 2018.

[4] K. B. Letaief, W. Chen, Y. Shi, J. Zhang, and Y.-J. A. Zhang, "The roadmap to 6G - AI empowered wireless networks," 2019. [Online]. Available: https://arxiv.org/abs/1904.11686

[5] E. Basar, M. Di Renzo, J. De Rosny, M. Debbah, M. Alouini, and R. Zhang, "Wireless communications through reconfigurable intelligent surfaces," *IEEE Access*, vol. 7, pp. 116 753–116 773, Aug. 2019.

[6] H. Yang *et al.*, "A programmable metasurface with dynamic polarization, scattering and focusing control," *Sci. Rep.*, vol. 6, Oct. 2016, Art. no. 35692.

[7] C. Liaskos, S. Nie, A. Tsioliaridou, A. Pitsillides, S. Ioannidis, and I. Akyildiz, "A new wireless communication paradigm through software-controlled metasurfaces," *IEEE Commun. Mag.*, vol. 56, no. 9, pp. 162–169, Sep. 2018.

[8] L. Yang, Y. Yang, M. O. Hasna, and M.-S. Alouini, "Coverage, Probability of SNR gain, and DOR analysis of RIS-Aided communication systems," *IEEE Wireless Commun. Lett.*, vol. 9, no. 8, pp. 1268–1272, Aug. 2020.

[9] M. H. Khoshafa, T. M. N. Ngatched, and M. H. Ahmed, "Reconfigurable intelligent surfaces-aided physical layer security enhancement in D2D underlay communications," *IEEE Commun. Lett.*, vol. 25, no. 5, pp. 1443–1447, May 2021.

[10] Z. Ding and H. Vincent Poor, "A simple design of IRS-NOMA transmission," *IEEE Commun. Lett.*, vol. 24, no. 5, pp. 1119–1123, May 2020.

[11] I. Trigui, W. Ajib, and W.-P. Zhu, "A comprehensive study of reconfigurable intelligent surfaces in generalized fading," 2020. [Online]. Available: https://arxiv.org/abs/2004.02922

[12] M. Badiu and J. P. Coon, "Communication through a large reflecting surface with phase errors," *IEEE Wireless Commun. Lett.*, vol. 9, no. 2, pp. 184–188, Feb. 2020.

[13] R. C. Ferreira, M. S. P. Facina, F. A. P. De Figueiredo, G. Fraidenraich, and E. R. De Lima, "Bit error probability for large intelligent surfaces under double-Nakagami fading channels," *IEEE Open J. Commun. Soc.*, vol. 1, pp. 750–759, May 2020.

[14] I. Trigui, E. K. Agbogla, M. Benjillali, W. Ajib, and W.-P. Zhu, "Bit error rate analysis for reconfigurable intelligent surfaces with phase errors," *IEEE Commun. Lett.*, vol. 25, no. 7, pp. 2176–2180, Jul. 2021.

[15] R. C. Ferreira, M. S. P. Facina, F. A. P. de Figueiredo, G. Fraidenraich, and E. R. de Lima, "Secrecy analysis and error probability of LIS-Aided communication systems under Nakagami-m fading," *Entropy*, vol. 23, no. 10, 2021, Art. no. 1284. [Online]. Available: https://www.mdpi.com/1099-4300/23/10/1284

[16] D. Selimis, K. P. Peppas, G. C. Alexandropoulos, and F. I. Lazarakis, "On the performance analysis of RIS-Empowered communications over Nakagami-m fading," *IEEE Commun. Lett.*, vol. 25, no. 7, pp. 2191–2195, Jul. 2021.
[17] Z. Zhang, Y. Cui, F. Yang, and L. Ding, "Analysis and optimization of outage probability in multi-intelligent reflecting surface-assisted systems," 2019. [Online]. Available: https://arxiv.org/abs/1909.02193
[18] X. Qian, M. D. Renzo, J. Liu, A. Kammoun, and M.-S. Alouini, "Beamforming through reconfigurable intelligent surfaces in single-user MIMO systems: SNR distribution and scaling laws in the presence of channel fading and phase noise," 2020. [Online]. Available: https://arxiv.org/abs/2005.07472
[19] S. A. Tegos, P. D. Diamantoulakis, A. S. Lioumpas, P. G. Sarigiannidis, and G. K. Karagiannidis, "Slotted ALOHA with NOMA for the next generation IoT," *IEEE Trans. Commun.*, vol. 68, no. 10, pp. 6289–6301, Oct. 2020.
[20] G. K. Karagiannidis, N. C. Sagias, and P. T. Mathiopoulos, "$N*$Nakagami: A. novel stochastic model for cascaded fading channels," *IEEE Trans. Commun.*, vol. 55, no. 8, pp. 1453–1458, Aug. 2007.
[21] I. S. Gradshteyn and I. M. Ryzhik, *Table of Integrals, Series, and Products*. New York, NY, USA: Academic Press, 2014.
[22] "The wolfram functions site." [Online]. Available: http://functions.wolfram.com
[23] M. Yacoub, G. Fraidenraich, and J. Santos Filho, "Nakagami-m phase-envelope joint distribution," *Electron. Lett.*, vol. 41, no. 5, pp. 259–261, Mar. 2005.
[24] K. V. Mardia and P. E. Jupp, *Directional Statistics*, vol. 494. Hoboken, NJ, USA: Wiley, 2009.
[25] M. Karlsson and E. G. Larsson, "On the operation of massive MIMO with and without transmitter CSI," in *Proc. IEEE 15th Int. Workshop Signal Process. Adv. Wireless Commun.*, Toronto, ON, Canada, 2014, pp. 1–5.
[26] V. S. Adamchik and O. I. Marichev, "The algorithm for calculating integrals of hypergeometric type functions and its realization in reduce system," in *Proc. Int. Symp. Symbolic Algebr. Comput.*, Tokyo, Japan, 1990, pp. 212–224.
[27] M. K. Simon and M.-S. Alouini, *Digital Communication Over Fading Channels*, 2nd ed. Hoboken, NJ, USA: Wiley, 2004.
[28] J. Lu, K. B. Letaief, J. C.-I. Chuang, and M. L. Liou, "M-PSK and M-QAM BER computation using signal-space concepts," *IEEE Trans. Commun.*, vol. 47, no. 2, pp. 181–184, Feb. 1999.
[29] M. K. Simon and M.-S. Alouini, *Digital Communication Over Fading Channels*. Hoboken, NJ, USA: Wiley, 2005.
[30] O. S. Badarneh, P. C. Sofotasios, S. Muhaidat, S. L. Cotton, and D. B. Da Costa, "Product and ratio of product of fisher-snedecor F. Variates and their applications to performance evaluations of wireless communication systems," *IEEE Access*, vol. 8, pp. 215 267–215 286, 2020.
[31] A. S. Lioumpas, G. K. Karagiannidis, and A. C. Iossifides, "Channel quality estimation index (CQEI): A long-term performance metric for fading channels and an application in EGC receivers," *IEEE Trans. Wireless Commun.*, vol. 6, no. 9, pp. 3315–3323, Sep. 2007.
[32] Q. Wu and R. Zhang, "Intelligent reflecting surface enhanced wireless network via joint active and passive beamforming," *IEEE Trans. Wireless Commun.*, vol. 18, no. 11, pp. 5394–5409, Nov. 2019.
[33] A. Abdi, H. Hashemi, and S. Nader-Esfahani, "On the PDF of the sum of random vectors," *IEEE Trans. Commun.*, vol. 48, no. 1, pp. 7–12, Jan. 2000.
[34] G. K. Karagiannidis, "A closed-form solution for the distribution of the sum of Nakagami-m random phase vectors," *IEEE Commun. Lett.*, vol. 10, no. 12, pp. 828–830, Dec. 2006.
[35] M. Abramowitz and I. Stegun, *Handbook of Mathematical Functions: With Formulas, Graphs, and Mathematical Tables, Ser. Applied Mathematics Series*. New York, NY, USA: Dover, 1965. [Online]. Available: https://books.google.gr/books?id=MtU8uP7XMvoC

Sotiris A. Tegos (Student Member, IEEE) received the Diploma (five years) in electrical and computer engineering in 2017 from the Aristotle University of Thessaloniki, Thessaloniki, Greece, where he is currently working toward the Ph.D. degree with the Department of Electrical and Computer Engineering. He is a Member of the Wireless Communications and Information Processing (WCIP) Group. In 2018, he was a Visitor Researcher with the Department of Electrical and Computer Engineering, Khalifa University, Abu Dhabi,United Arab Emirates. His research interests include wireless power transfer, probability theory and multiple access in wireless communications. He was an Exemplary Reviewer in *IEEE Wireless Communications Letters* for 2019 (top 3% of reviewers).

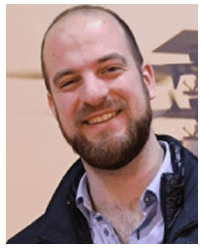

Dimitrios Tyrovolas (Student Member, IEEE) received the Diploma (five years) in electrical and computer engineering from the University of Patras, Patras, Greece, in 2020. He is currently working toward the Ph.D. degree with the Department of Electrical and Computer Engineering, Aristotle University of Thessaloniki, Thessaloniki, Greece. He is also a Member of the Wireless Communications and Information Processing (WCIP) Group. His research interests include reconfigurable intelligent surfaces, unmanned aerial vehicle communications, massive machine type communications and probability theory. He was an Exemplary Reviewer in IEEE Wireless Communications Letters for 2021 (top 3% of reviewers).

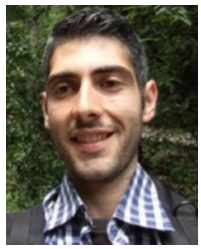

Panagiotis D. Diamantoulakis (Senior Member, IEEE) received the Diploma (five years) and the Ph.D. degree from the Department of Electrical and Computer Engineering, Aristotle University of Thessaloniki, Thessaloniki, Greece, in 2012 and 2017, respectively. Since 2017, he has been a Postdoctoral Fellow with Wireless Communications & Information Processing (WCIP) Group, AUTH and since 2021, he has been a Visiting Assistant Professor with the Key Lab of Information Coding and Transmission, Southwest Jiaotong University, Chengdu, China. His research interests include optimization theory and applications in wireless networks and smart grids, game theory, and optical wireless communications. He is the Editor of IEEE Wireless Communications Letters, *IEEE Open Journal of the Communications Society, Physical Communications* (Elsevier), and *Frontiers in Communications and Networks*.

Christos K. Liaskos (Member, IEEE) received the Diploma in electrical engineering from the Aristotle University of Thessaloniki (AUTH), Thessaloniki, Greece, in 2004, the M.Sc. degree in medical informatics from the Medical School, AUTH, in 2008, and the Ph.D. degree in computer networking from the Department of Informatics, AUTH, in 2014. He is currently an Assistant Professor with the University of Ioannina, Ioannina, Greece, and a FORTH affiliated Researcher. His research interests include computer networks, traffic management and novel schemes for wireless channel engineering.

George K. Karagiannidis (Fellow, IEEE) received the Diploma (five years) and Ph.D. degree, in electrical and computer engineering from the University of Patras, Patras, Greece, in 1987 and 1999, respectively. He is currently a Professor with Electrical and Computer Engineering Department and the Head of Wireless Communications & Information Processing (WCIP) Group. He is also a Honorary Professor with South West Jiaotong University, Chengdu, China. His research interests include digital communications systems and signal processing. He is currently an Associate Editor-in Chief of IEEE Open Journal of Communications Society. He is one of the highly-cited authors across all areas of Electrical Engineering, recognized from Clarivate Analytics as Web-of-Science Highly-Cited Researcher during 2015–2021. Prof. Karagiannidis was the recipient of the 2021 IEEE Communications Society Radio Communications Committee Technical Recognition Award and the 2018 Signal Processing and Communications Electronics Technical Recognition Award of the IEEE Communications Society.